Room temperature upconversion electroluminescence from a mid-infrared In(AsN) tunneling diode

D. M. Di Paola (iD), Q. Lu, E. Repiso, M. Kesaria (iD), O. Makarovsky (iD), A. Krier (iD), and A. Patanè (iD)

open access

View Online   Export Citation   CrossMark

ARTICLES YOU MAY BE INTERESTED IN

High-speed III-V based avalanche photodiodes for optical communications—the forefront and expanding applications
Applied Physics Letters 116, 140502 (2020); https://doi.org/10.1063/5.0003573

Mid-infrared dual-comb spectroscopy with room-temperature bi-functional interband cascade lasers and detectors
Applied Physics Letters 116, 141102 (2020); https://doi.org/10.1063/1.5143954

MOCVD growth of InP-based $1.3\mu m$ quantum dash lasers on (001) Si
Applied Physics Letters 116, 142106 (2020); https://doi.org/10.1063/1.5145031

AIP Publishing

Room temperature upconversion electroluminescence from a mid-infrared In(AsN) tunneling diode

D. M. Di Paola,[1,2,a)] (iD) Q. Lu,[3] E. Repiso,[3] M. Kesaria,[3] (iD) O. Makarovsky,[1] (iD) A. Krier,[3] (iD) and A. Patanè[1] (iD)

AFFILIATIONS

[1]School of Physics and Astronomy, University of Nottingham, Nottingham NG7 2RD, United Kingdom
[2]Department of Physics and Astronomy, The University of Sheffield, Sheffield S3 7RH, United Kingdom
[3]Physics Department, Lancaster University, Lancaster LA1 4YB, United Kingdom

[a)]Author to whom correspondence should be addressed: d.m.dipaola@sheffield.ac.uk

ABSTRACT

Light emitting diodes (LEDs) in the mid-infrared (MIR) spectral range require material systems with tailored optical absorption and emission at wavelengths $\lambda > 2\,\mu m$. Here, we report on MIR LEDs based on In(AsN)/(InAl)As resonant tunneling diodes (RTDs). The N-atoms lead to the formation of localized deep levels in the In(AsN) quantum well (QW) layer of the RTD. This has two main effects on the electroluminescence (EL) emission. By electrical injection of carriers into the N-related levels, EL emission is achieved at wavelengths significantly larger than for the QW emission ($\lambda \sim 3\,\mu m$), extending the output of the diode to $\lambda \sim 5\,\mu m$. Furthermore, for applied voltages well below the flatband condition of the diode, EL emission is observed at energies much larger than those supplied by the applied voltage and/or thermal energy, with an energy gain $\Delta E > 0.2$ eV at room temperature. We attribute this upconversion luminescence to an Auger-like recombination process.

The sensing of trace gases in the atmosphere represents a crucial technological challenge that requires the development of reliable light sources at target wavelengths. Many pollutants and gas species have their vibrational–rotational absorption bands in the mid-infrared (MIR) spectral range of the electromagnetic spectrum (wavelength $\lambda = 2$–$20\,\mu m$).[1–3] Thus, it is of paramount importance to develop materials and devices that can operate at these wavelengths. The MIR spectral range can be successfully covered by using different types of semiconductor lasers, such as quantum cascade lasers (QCLs)[4–6] or interband cascade lasers (ICLs),[7,8] providing robust and reliable systems for gas sensing. Despite being successfully developed, QCLs and ICLs are complex structures with prohibitive costs for widespread implementation. Consequently, there is merit in finding more cost-effective alternatives. MIR light emitting diodes (LEDs) represent attractive candidates, given their lower complexity, robustness, and lower power consumption, well suited for low-budget portable instrumentation.[9] However, apart from recent reports of interband cascade light emitting diodes (ICLEDs),[10–12] the room temperature output power of MIR LEDs tends to decrease for $\lambda > 2\,\mu m$. This low performance of MIR sources arises from a generally low radiative efficiency

due to thermal excitation of carriers and non-radiative Auger recombination.[13,14]

Among materials that operate in the MIR, III–V semiconductor compounds and their alloys have attracted great interest.[14–16] In particular, the direct narrow energy bandgap of InAs ($E_g = 0.415$ eV or $\lambda \sim 3\,\mu m$ at a temperature $T = 4.2$ K)[17] can be engineered by the controlled incorporation of nitrogen (N) atoms in the group-V sublattice. For example, by increasing the N-content by up to [N] = 3%, the bandgap can be reduced by $\sim$25%.[18,19] The N-incorporation also creates zero-dimensional states in the forbidden bandgap that are localized on nanometer length-scales.[20] In this work, we report on the room temperature operation of a resonant tunneling diode (RTD) based on the dilute nitride alloy In(AsN) as a MIR emitter. We show that the formation of deep N-related states in the bandgap of In(AsN) enables the recombination of carriers at energies significantly lower than the bandgap energy, extending the diode emission to $\lambda \sim 5\,\mu m$ at $T < 100$ K. The presence of strongly localized deep states also contributes to upconversion luminescence (UCL), i.e., electroluminescence (EL) emission at energies much larger than those supplied by the applied voltage and/or thermal energy, with an energy gain $\Delta E > 0.2$ eV at room temperature.
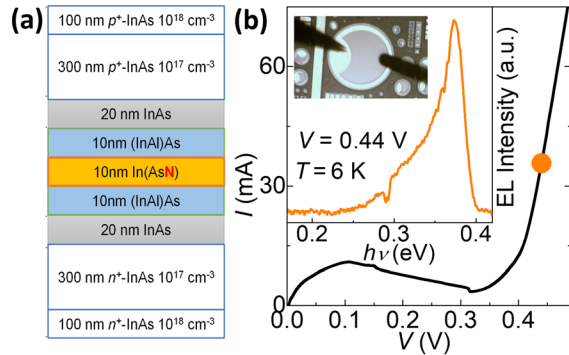
FIG. 1. (a) Layer structure of the In(AsN)/(InAl)As *p–i–n* RTD. (b) Current–voltage, *I*(*V*), curve at *T* = 6 K for an In(AsN) RTD with mesa diameter *d* = 800 μm. Inset: electroluminescence (EL) spectrum at an applied voltage *V* = 0.44 V, corresponding to the point of the *I*(*V*) indicated by the orange dot; optical image of the mesa diode.

For these studies, we designed and grew by molecular-beam epitaxy (MBE) a series of In(AsN) RTDs with the same layer structure as that described in Ref. 20 and shown in Fig. 1(a). The active region of the RTD consists of a 10 nm-wide In(AsN) quantum well (QW), with N-content [N] = 1%, embedded between two 10 nm (InAl)As tunnel barriers. The samples were processed into circular optical mesa structures with Ohmic contacts alloyed to the top (*p*-) and bottom (*n*-) doped InAs layers. Figure 1(b) shows the low temperature (*T* = 6 K) current–voltage, *I*(*V*), characteristics of the diode. In the following, we define a positive bias with the top *p*-type layer biased positive. For small positive applied biases, 0.1 V $\leq V \leq$ 0.3 V, the *I*(*V*) curve exhibits an extended region of negative differential resistance (NDR). This feature, commonly observed in Esaki diodes in forward bias,[21] is due to band-to-band Zener tunneling and involves the resonant transmission of electrons from the *n*- to the *p*-side of the diode through zero-dimensional N-related states in the QW layer.[20] For *V* > 0.3 V, the *I*(*V*) exhibits a conventional diode-like behavior. In this bias regime, the diode also emits EL [inset of Fig. 1(b)].

Figure 2 shows the EL spectra of an In(AsN)/(InAl)As RTD acquired at different applied voltages, *V*, and at temperatures, *T* = 6 K [Fig. 2(a)], *T* = 30 K [Fig. 2(b)], 100 K [Fig. 2(c)], and 300 K [Fig.

2(d)]. The inset in each figure shows the corresponding *I*(*V*) curve and the bias condition (colored dots) at which the EL spectra were acquired. At low temperatures [Figs. 2(a) and 2(b)] and *V* > 0.40 V, the EL spectra reveal two close bands at energies of *h*ν ~0.395 eV (peak I) and *h*ν ~0.375 eV (peak II), lower than that of the electron–hole recombination from the QW ground states (*h*ν ~0.43 eV). These EL emissions are weakly dependent on the voltage for *V* > 0.40 V. In contrast, for *V* < 0.40 V, the main EL emission has a strong dependence on the applied bias and, with decreasing *V*, it shifts to lower energies toward a broad band centred at *h*ν ~0.32 eV (band III). At intermediate temperatures [Fig. 2(c)], the EL spectrum shows the narrow high energy band I at *h*ν ~0.390 eV and the broader low energy band III between *h*ν ~ 0.27 eV and 0.35 eV. The EL peak positions of both bands I and III are weakly dependent on the applied bias. Finally, for *T* > 100 K [Fig. 2(d)], the intensity of band III weakens with increasing *T*. Band I is dominant at high *T* and its position does not depend on the applied voltage. Also, its energy decreases with increasing *T*, following the temperature dependence of the bandgap energy (supplementary material S1).

To probe further the origin the EL emission at different applied voltages and/or temperatures, we plot in Fig. 3 the color maps of the normalized EL intensity vs voltage, *V*, and photon energy, *h*ν, at *T* = 6 K [Fig. 3(a)], 100 K [Fig. 3(b)], and 300 K [Fig. 3(c)]. In each figure, we also show the corresponding *I*(*V*) curve. At *T* = 6 K [Fig. 3(a)], the *I*(*V*) shows an exponential diode-like increase in the current for biases above the flatband condition (*V* > 0.4 V) due to thermal diffusion of electrons (holes) from the *n*- (*p*-) to the *p*- (*n*-) side of the diode. Correspondingly, the EL emission is due to recombination of electrons from the QW ground states (peak I) or shallow donor states/clusters[22] (peak II) with holes in the QW ground state (supplementary material S2). For biases below the flatband condition (*V* < 0.4 V), the current arises mainly from Zener tunneling of electrons mediated by N-related defect states in the bandgap of In(AsN), giving rise to a strong NDR region.[20] Thus, the current is strongly suppressed and the EL emission occurs at lower energies, corresponding to the broad band III due to recombination of electrons from the N-related states[20] and holes from deep acceptor states.[22,23] From the color map in Fig. 3(a), it can be seen that band III occurs at energies *h*ν between *h*ν = *eV* − $\hbar\omega_{LO}$ and *h*ν = *eV* − 2$\hbar\omega_{LO}$, where $\hbar\omega_{LO}$ = 29 meV is the longitudinal optical (LO) phonon energy of InAs.[24,25] The
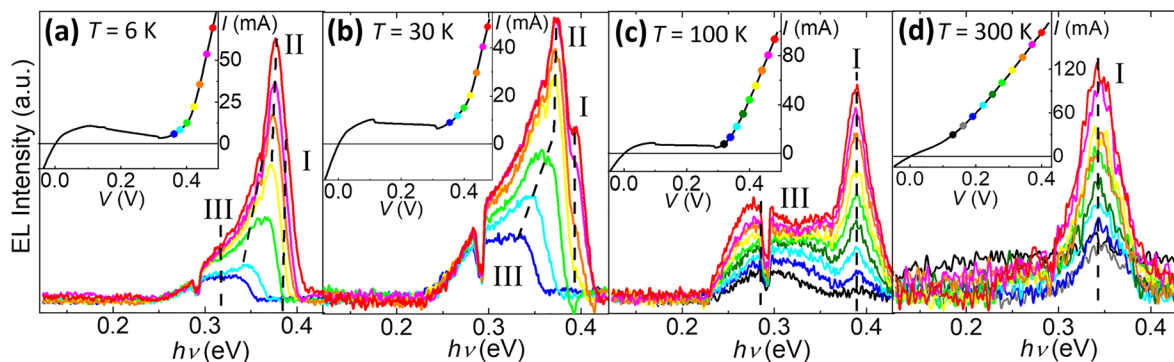

FIG. 2. EL spectra of an In(AsN)/(InAl)As RTD at different applied biases and at temperatures *T* = 6 K (a), 30 K (b), 100 K (c), and 300 K (d), showing bands I, II, and III. Inset: *I*(*V*) curves of the RTD. The colored dots on the *I*(*V*) indicate the voltages at which the corresponding EL spectra were acquired.
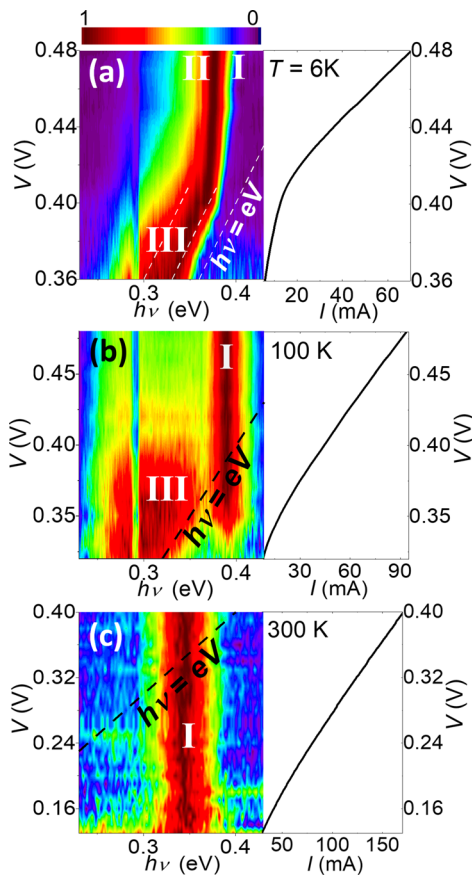
FIG. 3. Color maps of the normalized electroluminescence (EL) intensity vs voltage, V, and energy ($h\nu$) (left panels) and corresponding current–voltage, $I(V)$, curves (right panels) at $T = 6$ K (a), 100 K (b), and 300 K (c). Upconversion EL is observed at energies $h\nu > eV$.
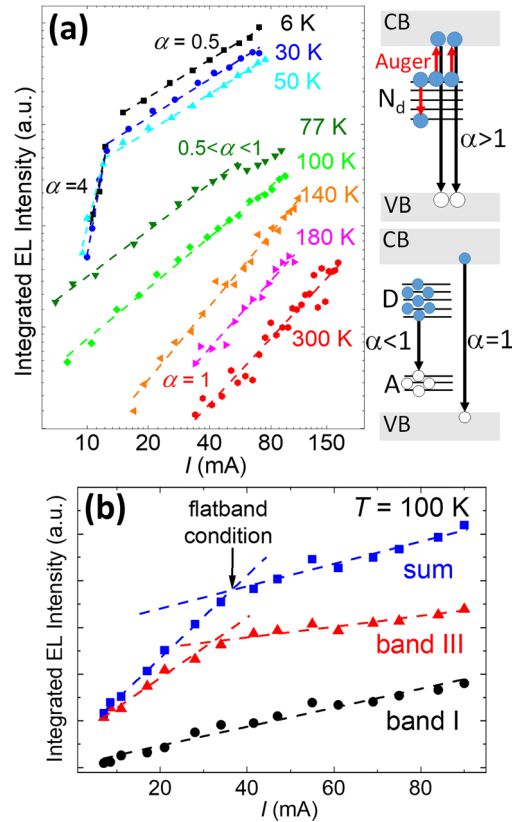

FIG. 4. Integrated intensity of the EL spectra as a function of the injection current, I, in a log–log scale, at $T = 6$–300 K. The scatters indicate the experimental data and the dashed lines represent the fits to the data by a power law with coefficient α. The sketches show examples of recombination in the superlinear ($\alpha > 1$), sublinear ($\alpha < 1$), and linear ($\alpha = 1$) regime. (b) Integrated EL intensity of the EL spectrum (blue squares), band I (black dots), and band III (red triangles) as a function of the injection current, I, in the linear scale, at $T = 100$ K.

contribution of defect-assisted Zener tunneling to the current becomes less dominant with increasing temperature. At $T = 100$ K [Fig. 3(b)] and $V < 0.40$ V, the broad band III can still be observed. However, the higher energy band I becomes dominant. Finally, at $T = 300$ K [Fig. 3(c)], a much higher current flows through the diode, leading to an EL emission (band I) whose energy position is weakly dependent on the applied voltage. Notably, we observe photon emission at energies higher than the excitation energy (i.e., in the range $h\nu > eV$). This phenomenon, also referred to as upconversion luminescence (UCL), has been reported in different systems.[26–28] Among semiconductors, it was observed in GaAs QWs,[29] InAs/GaAs self-assembled quantum dots (QDs)[30–33] and, more recently, in two-dimensional (2D) van der Waals materials[34,35] and heterostructures,[36] with an energy gain of up to 150 meV at room temperature.[37] In our RTDs, we observe UCL with a large energy gain $\Delta E > 200$ meV at $T = 300$ K.

We investigate the upconversion luminescence in our system by studying the dependence of the integrated EL intensity, EL_i, on the injection current, I, for temperatures in the range $T = 6$–300 K [Fig. 4(a)]. At low temperatures ($T = 6$–50 K), the data show a marked change in the dependence of EL_i on I at a characteristic

current, I_0, which corresponds to the flatband bias condition, V_0. For $V < V_0$, the dependence of EL_i on I is described by a power law, $EL_i \sim I^{\alpha}$, with $\alpha \sim 4$ for $V < V_0$ and $\alpha \sim 0.5$ for $V > V_0$. This change in the power law, I^{α}, around the flatband regime indicates a qualitative change in the injection of charge carriers into the In(AsN) QW. In particular, for $V < V_0$, carriers are injected into electronic states that lie below the conduction band edge of the In(AsN) layer. A superlinear behavior ($\alpha > 1$) can arise from the recombination of carriers via biexcitons, electron–hole plasmas, and/or Auger processes, as sketched in Fig. 4(a). A sublinear behavior ($\alpha < 1$) is instead suggestive of recombination of carriers from localized states that tend to saturate at high injection currents.[38–40] At intermediate temperatures ($T = 77$–100 K), the superlinear dependence of EL_i on I becomes weaker and the coefficient α takes values in the range $0.5 < \alpha < 1$. Since bands I and III can be better resolved at these temperatures, we plot in Fig. 4(b) their integrated EL intensity vs I (black dots and red triangles, respectively): it can be seen that the change in slope is observed only for band III (red dots). Finally, for $T > 100$ K, we find that $\alpha = 1$, corresponding to recombination of free excitons (band I)
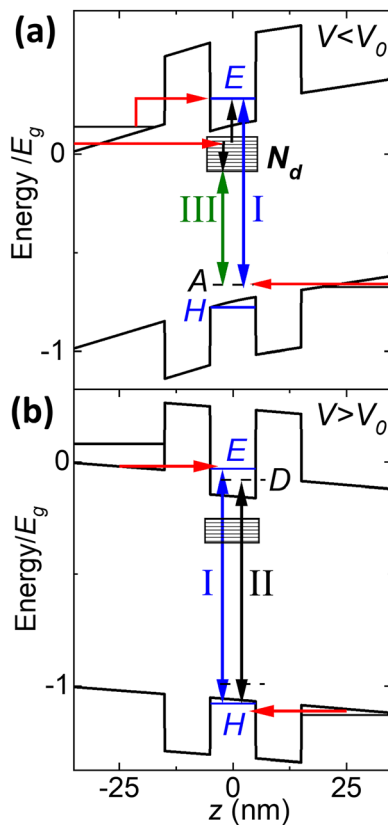
FIG. 5. Energy band diagrams, normalized to the energy bandgap, E_g, below (a) and above (b) flatband conditions, V_0. The EL emission arises from the recombination of carriers on QW states (I) shallow donors (II), and N-related defects, N_d (III).

and consistent with the T-dependence of the peak energy for band I (supplementary material S1).

The range of values for α suggests that different carrier recombination mechanisms are responsible for the EL emission at low ($T < 50$ K) and high ($T > 100$ K) temperatures.[38–40] We consider the band alignment of the RTD in Fig. 5 to describe these mechanisms. Details of the modeling are given in the supplementary material S2. In Fig. 5(a), we plot the calculated band diagram for an applied bias below the flatband condition of the diode ($V < V_0$). Under this condition, the emitter states are not resonant with the QW bound states. However, electrons can tunnel from the emitter into the N-related localized states in the bandgap (N_d). Following the emission of one or two LO phonons, they can then recombine with holes in acceptor (A) states, resulting in band III at energies significantly lower than the electron–hole recombination energy in the QW [see band III in Figs. 3(a) and 3(b)]. The EL spectra of the RTD and their bias dependence differ from those for the N-free sample: the N introduces a redshift of the free exciton EL emission by ∼25 meV; furthermore, it introduces localized states within the forbidden gap leading to a broader EL emission at longer wavelengths (supplementary material S3 and S4). Furthermore, as sketched in Fig. 5(a), electrons can be promoted from the N_d to the QW states through Auger recombination of non-equilibrium carriers. Auger recombination processes occur when the

energy arising upon the relaxation of an electron (hole) from an excited level is transferred to another electron (hole), the latter being promoted to a higher excited state.[41] These processes have been shown to be relevant for the carrier dynamics and recombination in several III–V confined semiconductor systems[42–44] and become prominent in the high-injection regime, when high carrier densities are achieved in localized states.[32,33] In our case, Auger-processes may be facilitated by strong Coulomb interactions between carriers confined in zero-dimensional N-related states. With increasing temperature, electrons can gain sufficient thermal energy to be excited from the N-levels into the QW. Thus, an increasing contribution of UCL at energies $h\nu > eV$ can be observed at low applied biases [see band I in Figs. 3(b) and 3(c)]. Finally, for an applied voltage above the flatband condition [Fig. 5(b)], electrons in the emitter states can tunnel resonantly into the QW bound electron state (E) or shallow donor levels (D), from which they recombine with holes injected from the collector into the QW ground state (H) or deep acceptor states (A). The injection can be assisted by the emission or absorption of an LO phonon. In this bias regime, the EL emission is dominated by band II (donor–acceptor recombination at low T) and by band I (free electron–acceptor recombination). The latter becomes dominant at a high T due to the ionization of the donors.

In summary, we have reported on EL studies of In(AsN)/ (InAl)As RTDs with emission in the MIR wavelength range $\lambda = 3$–5 μm. We have demonstrated a bias-tuneable EL emission at energies considerably lower that the bandgap energy of In(AsN) at a low temperature ($T = 6$–50 K). We attributed this behavior to the presence of N-related localized states below the conduction band minimum of In(AsN). The transmission of electrons into these states enables the recombination of carriers at energies below the bandgap energy, extending the EL emission toward longer wavelengths, up to $\lambda \sim 5$ μm. The observation of N-related localized defect states in the bandgap of In(AsN) raises new questions of fundamental and technological interest. Such defect states may have a strong influence on the opto-electronic properties of devices and the identification of their origin and nature requires further studies. In particular, a comprehensive theoretical model should include complex N-configurations and interstitial-N.[45–47] Further research may include the study of the EL output from RTDs with different N-contents and/or QW designs to extend the EL emission range to longer wavelengths ($\lambda > 5$ μm). Auger-assisted up-converted MIR luminescence with high energy gain at room temperature shows potential for applications in MIR photonics and low-budget MIR LEDs. The efficiency of these prototype devices (∼0.01%) could be significantly improved by using an antireflection coating, better heat sinking, and a grid contact geometry for current spreading.

See the supplementary material for the T-dependence of the EL emission spectra (S1), the modeling of the band structure of the RTDs (S2), and the EL studies of N-free InAs RTDs (S3).

AUTHOR'S CONTRIBUTIONS

D.M.D.P., O.M., A. K., and A.P. designed the experiments; D.M.D.P., Q.L., and E.R. performed the experiments; M.K. and A.K. grew the samples; D.M.D.P. and A.P. wrote the paper and all authors took part in the discussion and analysis of the data.

The authors declare that they have no competing financial interest.

REFERENCES

[1]T. Töpfer, K. P. Petrov, Y. Mine, D. Jundt, R. F. Curl, and F. K. Tittel, Appl. Opt. **36**, 8042 (1997).

[2]A. Kosterev, G. Wysocki, Y. Bakhirkin, S. So, R. Lewicki, M. Fraser, F. Tittel, and R. F. Curl, Appl. Phys. B **90**, 165 (2008).

[3]F. B. Barho, F. Gonzalez-Posada, M. J. Milla, M. Bomers, L. Cerutti, and T. Taliercio, Opt. Express **24**, 16175 (2016).

[4]F. Capasso, Opt. Eng. **49**, 111102 (2010).

[5]J. Faist, *Quantum Cascade Lasers* (Oxford University Press, Oxford, 2013).

[6]A. Tredicucci, R. Köhler, L. Mahler, H. E. Beere, E. H. Linfield, and D. A. Ritchie, Semicond. Sci. Technol. **20**, S222 (2005).

[7]S. Höfling, R. Weih, M. Dallner, and M. Kamp, *Interband Cascade Lasers for the Mid-Infrared Spectral Region*, SPIE OPTO ed. (SPIE, 2014), Vol. 9002, p. 6.

[8]R. Meyer, I. Vurgaftman, R. Q. Yang, and L. R. Ram-Mohan, Electron. Lett. **32**, 45 (1996).

[9]A. Krier, M. Yin, V. Smirnov, P. Batty, P. J. Carrington, V. Solovev, and V. Sherstnev, Phys. Status Solidi A **205**, 129 (2008).

[10]R. J. Ricker, S. R. Provence, D. T. Norton, T. F. Boggess, Jr., and J. P. Prineas, Appl. Phys. Lett. **121**, 185701 (2017).

[11]A. J. Muhowski, R. J. Ricker, T. F. Boggess, and J. P. Prineas, Appl. Phys. Lett. **111**, 243509 (2017).

[12]Y. Zhou, Q. Lu, X. Chai, Z. Xu, J. Chen, A. Krier, and L. He, Appl. Phys. Lett. **114**, 253507 (2019).

[13]K. O'Brien, S. J. Sweeney, A. R. Adams, S. R. Jin, C. N. Ahmad, B. N. Murdin, A. Salhi, Y. Rouillard, and A. Joullié, Phys. Status Solidi B **244**, 203 (2007).

[14]A. Krier, M. de la Mare, P. J. Carrington, M. Thompson, Q. Zhuang, A. Patanè, and R. Kudrawiec, Semicond. Sci. Technol. **27**, 094009 (2012).

[15]K. Ueno, E. G. Camargo, T. Katsumata, H. Goto, N. Kuze, Y. Kangawa, and K. Kakimoto, Jpn. J. Appl. Phys., Part 1 **52**, 092202 (2013).

[16]E. Delli, V. Letka, P. D. Hodgson, E. Repiso, J. P. Hayton, A. P. Craig, Q. Lu, R. Beanland, A. Krier, A. R. J. Marshall, and P. J. Carrington, ACS Photonics **6**, 538 (2019).

[17]Z. M. Fang, K. Y. Ma, D. H. Jaw, R. M. Cohen, and G. B. Stringfellow, J. Appl. Phys. **67**, 7034 (1990).

[18]Q. Zhuang, A. Godenir, and A. Krier, J. Phys. D **41**, 132002 (2008).

[19]R. Kudrawiec, J. Misiewicz, Q. Zhuang, A. M. R. Godenir, and A. Krier, Appl. Phys. Lett. **94**, 151902 (2009).

[20]D. M. Di Paola, M. Kesaria, O. Makarovsky, A. Velichko, L. Eaves, N. Mori, A. Krier, and A. Patanè, Sci. Rep. **6**, 32039 (2016).

[21]L. Esaki, Phys. Rev. **109**, 603 (1958).

[22]O. Madelung, *Semiconductors: Data Handbook* (Springer, Berlin, Heidelberg, 2004).

[23]O. A. Allaberenov, N. V. Zotova, D. N. Nasledov, and L. D. Neumina, Sov. Phys.-Semicond. **4**, 1662 (1973).

[24]S. Buchner and E. Burstein, Phys. Rev. Lett. **33**, 908 (1974).

[25]D. J. Lockwood, G. Yu, and N. L. Rowell, Solid State Commun. **136**, 404 (2005).

[26]E. Finkeißen, M. Potemski, P. Wyder, L. Viña, and G. Weimann, Appl. Phys. Lett. **75**, 1258 (1999).

[27]F. Auzel, Chem. Rev. **104**, 139 (2004).

[28]A. G. Joly, W. Chen, D. E. McCready, J.-O. Malm, and J.-O. Bovin, Phys. Rev. B **71**, 165304 (2005).

[29]S. Eshlaghi, W. Worthoff, A. Wieck, and D. Suter, Phys. Rev. B **77**, 245317 (2008).

[30]P. P. Paskov, P. O. Holtz, B. Monemar, J. M. Garcia, W. V. Schoenfeld, and P. M. Petroff, Appl. Phys. Lett. **77**, 812 (2000).

[31]C. Kammerer, G. Cassabois, C. Voisin, C. Delalande, P. Roussignol, and J. M. Gérard, Phys. Rev. Lett. **87**, 207401 (2001).

[32]L. Turyanska, A. Baumgartner, A. Chaggar, A. Patanè, L. Eaves, and M. Henini, Appl. Phys. Lett. **89**, 092106 (2006).

[33]A. Baumgartner, A. Chaggar, A. Patanè, L. Eaves, and M. Henini, Appl. Phys. Lett. **92**, 091121 (2008).

[34]A. M. Jones, H. Yu, J. R. Schaibley, J. Yan, D. G. Mandrus, T. Taniguchi, K. Watanabe, H. Dery, W. Yao, and X. Xu, Nat. Phys. **12**, 323 (2016).

[35]M. Manca, M. M. Glazov, C. Robert, F. Cadiz, T. Taniguchi, K. Watanabe, E. Courtade, T. Amand, P. Renucci, X. Marie, G. Wang, and B. Urbaszek, Nat. Commun. **8**, 14927 (2017).

[36]J. Binder, J. Howarth, F. Withers, M. R. Molas, T. Taniguchi, K. Watanabe, C. Faugeras, A. Wysmolek, M. Danovich, V. I. Fal'ko, A. K. Geim, K. S. Novoselov, M. Potemski, and A. Kozikov, Nat. Commun. **10**, 2335 (2019).

[37]J. Jadczak, L. Bryja, J. Kutrowska-Girzycka, P. Kapuściński, M. Bieniek, Y. S. Huang, and P. Hawrylak, Nat. Commun. **10**, 107 (2019).

[38]T. Schmidt, K. Lischka, and W. Zulehner, Phys. Rev. B **45**, 8989 (1992).

[39]L. Pavesi and M. Guzzi, J. Appl. Phys. **75**, 4779 (1994).

[40]E. F. Schubert, *Light-Emitting Diodes*, 2nd ed. (Cambridge University Press, Cambridge, 2006).

[41]A. R. Beattie and P. T. Landsberg, Proc. R. Soc. London., Ser. A **249**, 16 (1959).

[42]R. Ferreira and G. Bastard, Appl. Phys. Lett. **74**, 2818 (1999).

[43]D. Morris, N. Perret, and S. Fafard, Appl. Phys. Lett. **75**, 3593 (1999).

[44]F. Pulizzi, A. J. Kent, A. Patanè, L. Eaves, and M. Henini, Appl. Phys. Lett. **84**, 3046 (2004).

[45]I. A. Buyanova, W. M. Chen, and C. W. Tu, J. Phys. **16**, S3027 (2004).

[46]A. Lindsay and E. P. O'Reilly, Phys. Rev. Lett. **93**, 196402 (2004).

[47]W. M. Chen, I. A. Buyanova, C. W. Tub, and H. Yonezuc, Physica B **376-377**, 545 (2006).